Effect of microstructural evolution on magnetic property of Mn-implanted p -type GaN

Jeong Min Baik, Hyung Seok Kim, Chan Gyung Park, and Jong-Lam Lee

Citation: Applied Physics Letters **83**, 2632 (2003); doi: 10.1063/1.1615676

View online: http://dx.doi.org/10.1063/1.1615676

View Table of Contents: http://scitation.aip.org/content/aip/journal/apl/83/13?ver=pdfcov

Published by the AIP Publishing

Effect of microstructural evolution on magnetic property of Mn-implanted *p*-type GaN

Jeong Min Baik, Hyung Seok Kim, Chan Gyung Park, and Jong-Lam Lee[a)]
Department of Materials Science and Engineering, Pohang University of Science and Technology (POSTECH), Pohang, Kyungbuk 790-784, Korea

(Received 20 January 2003; accepted 1 August 2003)

The microstructural evolution of Mn-implanted *p*-type GaN has been studied using cross-sectional transmission electron microscopy. As Mn_3Ga nanoclusters (3–7 nm) with a hexagonal structure were produced by annealing ($\leqslant 800\,^{\circ}C$), the weak ferromagnetic property emerged. Higher-temperature annealing ($\geqslant 900\,^{\circ}C$) reduced the ferromagnetic signal and produced antiferromagnetic Mn-nitride nanoclusters, such as $Mn_6N_{2.58}$ and Mn_3N_2. This provides evidence that the ferromagnetic property was deeply related to microstructural changes of nanoclusters. © *2003 American Institute of Physics.* [DOI: 10.1063/1.1615676]

Dilute magnetic semiconductors (DMSs) based on III–V semiconductors have attracted great interest due to their potential applications in spintronics devices, such as spin-field effect transistors, and ultradense nonvolatile semiconductor memory.[1–4] Although ferromagnetism were discovered in (Ga,Mn)As and (In,Mn)As, their Curie temperatures (T_C) are still too low (<110 K) for industrial applications.[5,6]

It was theoretically suggested that (Ga,Mn)N with a high Mn concentration (~ 5 at. %) and a high hole concentration ($\sim 10^{20}$ cm^{-3}) could yield a high T_C ($\geqslant 300$ K).[7] Mn-doped GaN films showing ferromagnetic behavior were grown on sapphire (0001) by molecular beam epitaxy.[8] The ferromagnetic property was also reported in Mn-implanted GaN with subsequent annealing.[9] Based on x-ray diffraction (XRD) and/or transmission electron microscopy (TEM) analyses, it was proposed that the origin of ferromagnetism could be related to (Ga,Mn)N solid solution and/or Ga–Mn secondary phases. However, no detailed information on secondary phases, such as the crystal structure and composition, was experimentally provided. Furthermore, little was known about the change in magnetic property with the microstructural evolution of (Ga,Mn)N films. Synchrotron radiation x-ray scattering and field-emission TEM (FE-TEM) with a high spatial resolution of 0.19 nm could provide the quantitative information about the microstrucural evolutions, which should be crucial for understanding the origin of ferromagnetic properties in the (Ga,Mn)N.

In this work, we studied microstructural evolution of Mn-implanted *p*-type GaN as a function of annealing temperature. Secondary ion mass spectrometry analysis was performed to get the depth distribution of Mn, Ga, O, and N atoms. The FE-TEM and synchrotron XRD were employed for the structural characterization. The magnetization properties were characterized using a superconducting quantum interference device magnetometer (MPMSXL, Quantum Design Co., Ltd). Based on these studies, we present the relationship between the microstructural evolution and the change of magnetic properties.

The GaN films used in this work were grown by metal-organic chemical deposition on a (0001) sapphire substrate. An undoped GaN layer with a thickness of 1 μm was grown, followed by a growth of 1-μm-thick *p*-type GaN doped with Mg. Electrical activation of the grown samples was carried out at 750 °C for 4 min by rapid thermal annealing (RTA) under a N_2 atmosphere. Net hole concentration in the film was determined to be 2.5×10^{17} cm^{-3} by Hall measurements. After growing the film, Mn^+ ions were implanted with an energy of 180 keV and dose of 5×10^{16} cm^{-2} to an produce average volume concentration of 5 at. % in the GaN films. All samples were held at 350 °C during the implantation to avoid amorphization. Subsequent annealing at 700–900 °C for 30 s was performed under a flowing N_2 gas in a face-to-face condition. For measurement of the resistivity, the samples were patterned using the transmission line method with 100×50 μm^2 pads. Ti/Al/Ni/Au (300 Å/1200 Å/400 Å/500 Å) contact was annealed under flowing N_2 at 500 °C for 1 min using RTA.

Magnetic properties of Mn-implanted sample with annealing temperature were shown in Fig. 1. The magnetization data were obtained with the applied field parallel to the plane of the samples. The diamagnetic background of GaN sub-

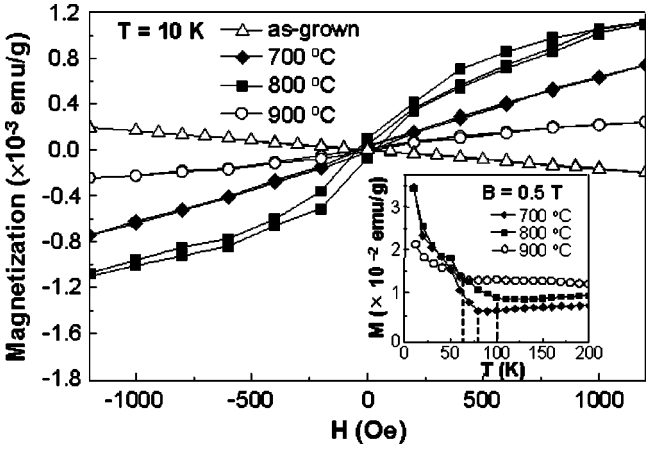

FIG. 1. Magnetization curves for as-grown sample and Mn-implanted samples with annealing temperature. The inset shows the temperature dependence of magnetization with annealing temperature.

a)Electronic mail: jllee@postech.ac.kr

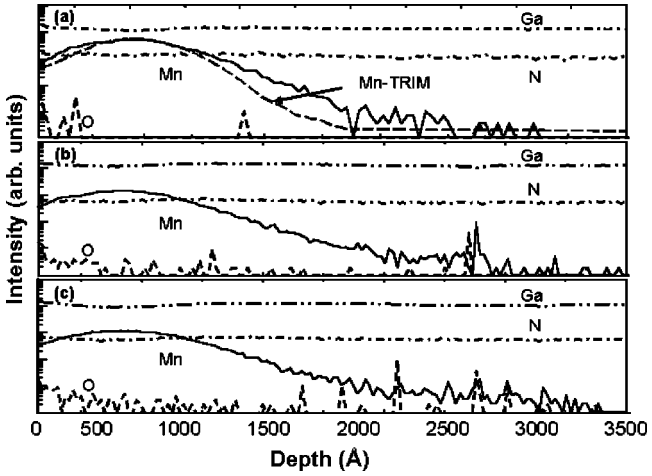

FIG. 2. Depth profiles of Mn, Ga, N, and O atoms for Mn-implanted samples: (a) As-implanted, (b) after annealing at 800 °C, and (c) 900 °C. TRIM simulated atomic profile of implanted Mn atoms was also shown in as-implanted sample.

strate was carefully measured and subtracted from the magnetization measurements. When compared to the substrate, hysteresis loops are clearly apparent in the Mn-implanted samples with subsequent annealing. The coercive field (H_C) increased from 21 to 79 Oe with annealing temperature. However, the residual magnetization (M_R) was the highest for 800-°C-annealed sample. The temperature dependence of magnetization in a magnetic field ($B=0.5$ T) showed a ferromagnetic behavior persisting to 100 K. Even though T_C is low in comparison with the reported values,[8,9] it is clear that the highest T_C (100 K) is obtained after annealing at 800 °C.

Figure 2 shows the depth profiles of Mn, Ga, N, and O atoms as a function of annealing temperature. For the as-implanted sample, the experimentally determined peak position of implanted Mn atoms is in good agreement with the result calculated by transport of ions in matter (TRIM), as shown in Fig. 1(a). As the annealing temperature increased, the implanted Mn atoms were slightly diffused, but it was independent of the annealing temperature. Only a small amount of O atoms were detected in the as-implanted sample, and no more increase in O amount was found even after annealing. This means that the magnetic property of

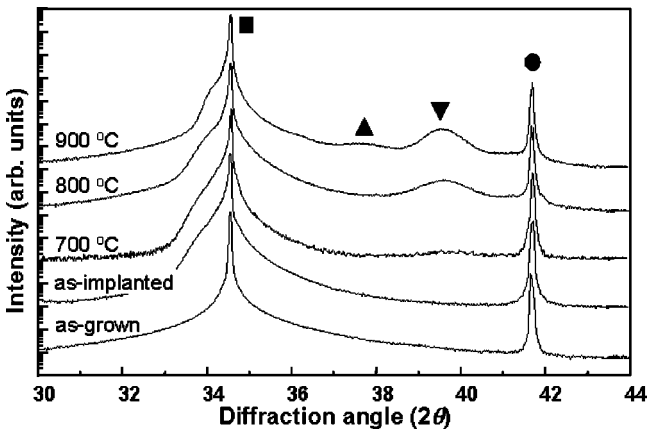

FIG. 3. Change of XRD scans for the Mn-implanted GaN with the annealing temperature: (■) GaN, (●) Al_2O_3, (▼) $Mn_6N_{2.58}$, (▲) Mn_3N_2.

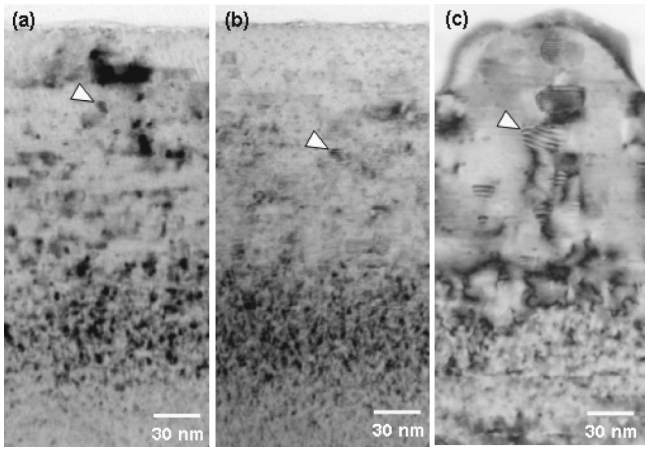

FIG. 4. Cross-sectional bright-field TEM images of the Mn-implanted GaN as a function of annealing temperature: (a) 700 °C, (b) 800 °C, and (c) 900 °C.

Mn-implanted sample in Fig. 1 was independent of O incorporation in GaN.

Figure 3 shows XRD profiles of Mn-implanted GaN samples with annealing temperature. In the as-implanted sample, no reaction between Mn and GaN was observed. After annealing at 700 °C, the Mn–N binary phase of $Mn_6N_{2.58}$ was produced. The $Mn_6N_{2.58}$ peak intensity increased with the annealing temperature. When the sample was annealed at 900 °C, a peak corresponding to Mn_3N_2 was observed. A shoulder was found at the lower angle side of GaN (0002) peak and its intensity became large at a higher annealing temperature. The shoulder could attribute to the strain along the GaN *c* axis, resulting from the decrease in implantation-induced damage during the annealing.[10]

Figure 4 shows cross-sectional TEM images of the Mn-implanted GaN samples with annealing temperature. After annealing at 700 °C, nanoclusters with moiré fringe were formed, as shown in Fig. 4(a). The cluster size ranged from 3 to 7 nm. The increase in the cluster size in the 800 °C annealed samples is little in comparison with the 700 °C annealed one. When the annealing temperature increased to 900 °C, the cluster size increased to around 30 nm.

Figure 5 shows the high-resolution images and diffraction patterns for both the 700- and 900-°C-annealed samples. In the 700-°C-annealed sample, a number of clusters with a few nanometers were found in the GaN matrix. The interface

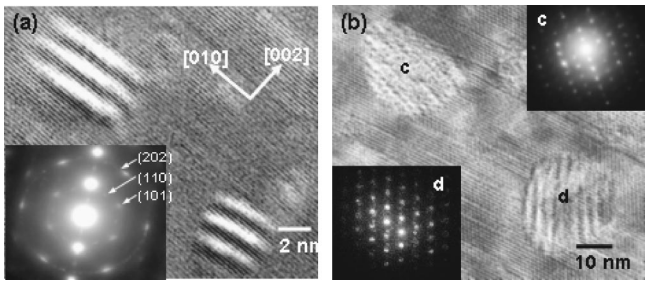

FIG. 5. High-resolution TEM image and SADPs for Mn-implanted and annealed GaN samples: (a) The annealing temperature was 700 °C. The SADPs in the inset support that the phase corresponds to Mn_3Ga. (b) High-resolution image and nanobeam diffraction patterns for the 900-°C-annealed sample. The nanobeam diffraction patterns of the phase marked as **c** and **d** correspond to $Mn_6N_{2.58}$ and Mn_3N_2, respectively.

TABLE I. Resistivity of the Ti/Al/Ni/Au contact on Mn-implanted samples with annealing temperature.

Annealing temperature (°C)	Resistivity (Ω cm)
700	48.11
800	8.96
900	10.37

of cluster with a matrix interface in the samples is not well defined. Using the identified phases from the diffraction patterns, the patterns obtained were indexed. The lattice parameter of the GaN substrate was used as a reference in indexing the phases. The interplanar spacings of the phases found at the area in Fig. 5(a) were calculated to be 3.195, 2.723, and 1.581 Å by the selected area diffraction patterns (SADPs), which corresponds to the interplanar spacings of Mn_3Ga (101) ($d=3.189$ Å), (110) ($d=2.702$ Å), and (202) ($d=1.5945$ Å), respectively. Thus, the diffraction patterns revealed that crystallites correspond to Mn_3Ga with typical hexagonal structure. The nanoclusters were also observed in 800-°C-annealed samples. After annealing at 900 °C, a well-defined cluster/matrix interface was revealed, as shown in Fig. 5(b). The nanobeam diffraction patterns of the phase marked as "**c**," observed along the [2-11] zone direction in a hexagonal structure, were displayed in the inset of Fig. 5(b). The interplanar spacings of the phases were calculated to be 2.44 and 1.74 Å, which corresponds to the interplanar spacings of $Mn_6N_{2.58}$ (110) ($d=2.4455$ Å) and (112) ($d=1.6655$ Å). The interplanar spacing of 2.184 Å determined in the [001] zone direction of the region "**d**" corresponds to Mn_3N_2 (101) ($d=2.10$ Å). This presence of Mn nitrides is in good agreement with the XRD data in Fig. 3.

The resistivities of Mn-implanted samples with annealing temperature are summarized in Table I. After annealing at 800 °C, a minimum resisivity of approximately 8.96 Ω cm was measured. The decrease of resistivity could be explained as the enhancement in the crystallinity of the Mn-implanted samples. The increase of resistivity after annealing at 900 °C could be attributed to the decrease of the metallic Mn_3Ga phase. It was reported that the high conductive Mn_3GaN enhanced the conductivity of the GaMnN films.[11] Thus, it is suggested that the metallic Ga–Mn phase could increases the conductivity of the samples.

The observed weak ferromagnetic behaviors of the Mn-implanted samples can have several physical origins. The Mn_3Ga nanoclusters were mainly formed after annealing at 700 °C, as shown in Fig. 5(a). It was reported that a Mn_3Ga bulk material showed a weak ferromagnetism increasing below 100 K similarly to the magnetic data of the inset of Fig. 1.[12] Thus, the magnetic properties can be related to Mn_3Ga bulk properties. Meanwhile, Mn_3Ga nanoclusters can be superparamagnetic and induce hystersis below a blocking temperature, which can be also in the order of magnitude of 100 K. One other possibility is that Mn_3Ga clusters increase hole concentration by the formation of Ga vacancies, which coupled Mn spins randomly distributed in the GaN matrix. As the annealing temperature increased to 900 °C, the ferromagnetic property disappeared. No Mn_3Ga compounds were observed, but Mn nitrides, such as Mn_3N_2 and $Mn_6N_{2.58}$, were found. A number of N vacancies acting as donors for the electron could be produced by the formation of Mn nitrides, leading to the reduction of hole concentration. In addition, these Mn nitrides are known as antiferromagnetic materials with a Néel temperature above 300 K,[13,14] reducing the magnetic moment of the Mn-implanted GaN.

In conclusion, nanoclusters of Mn_3Ga (3–7 nm) with hexagonal structure were produced, generating Ga vacancies near the nanoclusters, when the Mn-implanted GaN was annealed at annealing temperatures lower than 800 °C. This reaction could cause an increase in the net hole concentration, resulting in the enhancement of a ferromagnetic property. At higher annealing temperatures ($\geqslant$900 °C), no Mn_3Ga compounds were observed, but Mn nitrides, such as Mn_3N_2 and $Mn_6N_{2.58}$, were found, implying the production of N vacancies. This resulted in the reduction of net hole concentration and, thereby, the decrease in the ferromagnetic property.

This work was supported in part by Korea Science and Engineering Foundation through the Quantum-functional Semiconductor Research Center at Dongguk University in 2003, and in part by the project for "National Research Laboratory" sponsored by the Korea Institute of Science and Technology Evaluation and Planning (KISTEP). High-resolution XRD using synchrotron radiation was carried out at the 3C2 beamline at Pohang Accelerator Laboratory.

[1] H. Ohno, Science **281**, 951 (1998).
[2] H. Ohno, A. Shen, F. Matsukura, A. Oiwa, A. Endo, S. Katsumoto, and Y. Iye, Appl. Phys. Lett. **69**, 363 (1996).
[3] S. A. Wolf, D. D. Awschalom, R. A. Buhrman, J. M. Daughton, S. von Molna, M. L. Roukes, A. Y. Chtchelkanova, and D. M. Treger, Science **294**, 1488 (2001).
[4] M. L. Reed, N. A. El-Masry, H. H. Stadelmaier, M. K. Ritums, M. J. Reed, C. A. Parker, J. C. Roberts, and S. M. Bedair, Appl. Phys. Lett. **79**, 3473 (2001).
[5] A. Oiwa, T. Slupinski, and H. Munekata, Appl. Phys. Lett. **78**, 518 (2001).
[6] K. Takamura, F. Matsukura, D. Chiba, and H. Ohno, Appl. Phys. Lett. **81**, 2590 (2002).
[7] T. Diel, H. Ohno, F. Matsukura, J. Cibert, and D. Ferrand, Science **287**, 1019 (2000).
[8] S. Sonoda, S. Shimizu, T. Sasaki, Y. Yamamoto, and H. Hori, J. Cryst. Growth **237**, 1358 (2002).
[9] N. Theodoropoulou, A. F. Hebard, M. E. Overberg, C. R. Abernathy, S. J. Pearton, S. N. G. Chu, and R. G. Wilson, Appl. Phys. Lett. **78**, 3475 (2001).
[10] B. J. Pong, C. J. Pan, Y. C. Teng, G. C. Chi, W.-H. Li, K. C. Lee, and C.-H. Lee, J. Appl. Phys. **83**, 5992 (1998).
[11] K. H. Kim, K. J. Lee, D. J. Kim, H. J. Kim, Y. E. Ihm, D. Djayaprawira, M. Takahashi, C. S. Kim, C. G. Kim, and S. H. Yoo, Appl. Phys. Lett. **82**, 1775 (2003).
[12] H. Niida, T. Hori, and Y. Nakagawa, J. Phys. Soc. Jpn. **52**, 1512 (1983).
[13] H. Yang, H. Al-Brithen, E. Trifan, D. C. Ingram, and A. R. Smith, J. Appl. Phys. **91**, 1053 (2002).
[14] M. N. Eddine and E. F. Bertaut, Solid State Commun. **23**, 147 (1977).